Current Optics and Photonics
Vol. 4, No. 1, February 2020, pp. 9-15

ISSN: 2508-7266(Print) / ISSN: 2508-7274(Online)
DOI: https://doi.org/10.3807/COPP.2020.4.1.009

Simulation of an X-ray Fresnel Zone Plate with Nonideal Factors

Jie Chen[1,2], Quanping Fan[3,4], Junhua Wang[1]*, Dengpeng Yuan[2], Lai Wei[3,4], Qiangqiang Zhang[3,4], Junsheng Liao[2], and Min Xu[1]*

[1]Shanghai Engineering Center of Ultra-precision Optical Manufacturing, Fudan University, Shanghai 200433, P. R. China
[2]Institute of Materials, China Academy of Engineering Physics, Mianyang 621907, P. R. China
[3]Research Center of Laser Fusion, China Academy of Engineering Physics, Mianyang 621900, P. R. China
[4]Science and Technology on Plasma Physics Laboratory, China Academy of Engineering Physics, Mianyang 621900, P. R. China

(Received June 21, 2019 : revised September 10, 2019 : accepted September 16, 2019)

Fresnel zone plates have been widely used in many applications, such as x-ray telescopes, microfluorescence, and microimaging. To obtain an x-ray Fresnel zone plate, many fabrication methods, such as electron-beam etching, ion-beam etching and chemical etching, have been developed. Fresnel zone plates fabricated by these methods will inevitably lead to some nonideal factors, which have an impact on the focusing characteristics of the zone plate. In this paper, the influences of these nonideal factors on the focusing characteristics of the zone plate are studied systematically, by numerical simulations based on scalar diffraction theory. The influence of the thickness of a Fresnel zone plate on the absolute focusing efficiency is calculated for a given incident x-ray's wavelength. The diffraction efficiency and size of the focal spot are calculated for different incline angles of the groove. The simulations of zone plates without struts, with regular struts, and with random struts are carried out, to study the effects of struts on the focusing characteristics of a zone plate. When a Fresnel zone plate is used to focus an ultrashort x-ray pulse, the effect of zone-plate structure on the final pulse duration is also discussed.

Keywords : Fresnel zone plate, Kirchhoff diffraction theory, Nonideal factors, Focusing characteristics, Numerical simulation
OCIS codes : (070.7345) Wave propagation; (050.1940) Diffraction; (230.3990) Micro-optical devices

I. INTRODUCTION

As the refractive index is very close to unity for all materials at x-ray wavelengths [1], an x-ray beam cannot be focused by refraction. The use of diffractive elements to realize x-ray focusing is an alternative method. Fresnel zone plates (FZPs) have been the most widely used diffractive elements for hard-x-ray focusing. Applications include synchrotrons, free-electron lasers, and other laboratory sources. FZPs can achieve very high spatial resolution [2]. Typically, an amplitude FZP consists of a series of alternating transparent and opaque concentric rings (zones) of prescribed radii [3]. A phase-shifting FZP has concentric rings causing alternating phase delay. Because it is efficient for the focusing of hard x-rays (photon energies above 8 keV) [4], a Fresnel zone plate with submicrometer dimensions has been used for purposes such as x-ray telescopes, micro-fluorescence, microimaging, microspectroscopy, and microdiffraction. In these applications the focusing of hard-x-ray beams is an important requirement for each experimental technique.

Spatial resolution and absolute focusing efficiency are two important parameters of an FZP. The diffraction limit of an FZP is associated with the smallest, outermost zone

*Corresponding author: wangjunhua@fudan.edu.cn, ORCID 0000-0002-0885-8234
minx@fudan.edu.cn, ORCID 0000-0002-4901-0088

Color versions of one or more of the figures in this paper are available online.

width. A nanolithography process with sufficient resolution has to be applied during fabrication. For an ideal FZP, analytical formulas have been developed to calculate the focusing efficiency, focal spot, and focal depth for a given incident wavelength. The focusing efficiency for an ideal amplitude FZP is about 10%, and about 40% for an ideal phase FZP [5]. The radius of the focal spot is $R = 1.22\Delta r$, and the Rayleigh length of the focal spot is $Z_L = \frac{4\pi R^2}{\lambda}$. At present, the main FZP fabrication techniques include e-beam lithography, ion-beam lithography, surface plasma chemical vacuum deposition, and wet (dry or metal-assisted) chemical etching [6-9]. There is always a difference between the structure of an FZP obtained by an actual fabrication process and that of an ideal FZP. Nonideal factors, such as sidewalls with incline angle [10] or metal struts [11], will inevitably be introduced. In addition, due to the strong penetration of hard x-rays [12], the incident x-ray pulse's duration will also affect the focusing properties of an actual FZP.

This paper presents numerical simulations to systematically study the influence of nonideal factors on the focusing properties of an FZP. The paper is arranged as follows: Section II introduces the theoretical methods of the numerical calculations; Section III discusses the influences of several nonideal factors on focusing properties; and Section IV presents the conclusions.

II. METHODS

The structure of a Fresnel zone plate, consisting of alternating transparent and opaque zones, is shown in Fig. 1. When a plane wave with a wavelength of λ is incident on the zone plate, it converges to a focal point after being focused by the zone plate. The focal length $f = \frac{r_1^2}{\lambda}$ is related to the wavelength of the incident light and the radius r_1 of the first zone of the plate. The focusing process of a Fresnel zone plate satisfies $f \gg r_N$, where r_N is the radius of the outermost zone. The focusing action of an FZP is far-field diffraction, which can be well simulated and analyzed by scalar diffraction theory. The focusing properties of the zone plate are numerically calculated by Kirchhoff diffraction theory [13]. In the case

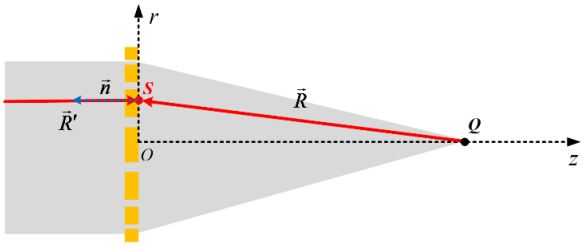

FIG. 1. Schematic diagram of a Fresnel zone plate.

of a plane wave, the complex amplitude of the diffraction field can be expressed as [14]:

$$U(Q) = \frac{A}{j\lambda}\exp(jkR') \cdot \iint_S t(S)\left[\frac{\cos(\vec{n},\vec{R}) - \cos(\vec{n},\vec{R'})}{2}\right]\frac{\exp(jkR)}{R}dS, \quad (1)$$

where A is a constant, $t(S)$ is the transmission function of the Fresnel zone plate, R' is the distance from a plane-wave front to a point S on the zone-plate aperture surface and $\vec{R'}$ is its unit vector, R is the distance from the observation point Q to a point S on the aperture surface and $\vec{R}$ is its unit vector, and $\vec{n}$ is the unit vector normal to the aperture surface. Assuming that the coordinates of point S are (x_0, y_0, 0) and those of point Q are (x_1, y_1, z_1), the transmittance function of an FZP can be expressed as $t(S) = t(x,y) = t(r,\theta)$, in which R' is a constant, $R = \overline{SQ} = \sqrt{(x_1-x_0)^2+(y_1-y_0)^2+z_1^2}$, and $dS = dxdy = rdrd\theta$. $z_1 = f$ is selected in the calculation of the focal plane. After $U(x_1, y_1)$ has been calculated by the numerical integral of Eq. (1), the intensity I(x_1, y_1) can be obtained by

$$I(x_1,y_1) = |U(x_1,y_1)|^2. \quad (2)$$

Using Eqs. (1) and (2), the focusing properties of the zone plate in the focusing region can be numerically calculated, as long as the transmission function of the FZP is determined. The focal-spot radius, focusing efficiency, and other information can also be obtained by simulations.

III. RESULTS

In the application of FZPs, there are often some nonideal factors, which lead to a great difference between the actual focusing properties and the ideal situation. For example, due to the strong penetration of hard x-rays, the influence of material absorption and phase shift caused by thickness is worth considering. The actual manufacturing errors in an FZP, such as step sidewall tilt, may also affect the focusing properties. To realize self-support of the zone plate's structure, the presence of intentionally added metal struts is not negligible. Since FZPs have been widely used in the focusing of ultrashort x-ray pulses, such as synchrotron radiation and free-electron lasers, the effect of the FZP's structure on the pulse duration of the focal spot is a valuable research issue.

3.1. The Effects of Film Thickness

The structure of an FZP for x-ray-focusing applications is shown in Fig. 2. The white areas are the structures of the opaque concentric rings, generally made using high-Z metal materials. Ideally the opaque concentric rings will completely obscure the x-rays, such that the transmittance

is zero. Due to the strong penetration of hard x-rays, though, they cannot be completely obscured by thin-film material having a thickness of several micrometers. X-rays penetrate the FZP with phase changes; therefore, the x-ray Fresnel zone plate may be regarded as a combination of a phase FZP and an amplitude FZP that simultaneously modulate the amplitude and phase of the incident light. The effects of material thickness on the focusing properties of an x-ray FZP are discussed below.

For hard x-rays, the refractive index of almost all materials tends to unity, so the refractive index can be expressed as $n=1-\delta+i\beta$. Considering the material absorption and phase shift of the x-rays, a transmission function for the whole FZP can be expressed as [15]:

$$\bar{t}(x,y)=t(x,y)+[1-t(x,y)]\cdot\exp\left(-j\cdot\frac{2\pi\delta}{\lambda}\tau\right)\cdot\exp\left(-\frac{2\pi\beta}{\lambda}\tau\right), \tag{3}$$

where β indicates the absorption coefficient of the FZP material, δ indicates its phase-shift coefficient, and τ indicates its thickness. From Eq. (3) we can see that different thicknesses τ of the FZPs will introduce different phase shifts $\exp\left(-j\cdot\frac{2\pi\delta}{\lambda}\tau\right)$ and different attenuations $\exp\left(-\frac{2\pi\beta}{\lambda}\tau\right)$ into the transmittance function $\bar{t}(x,y)$, ultimately leading to different values of focusing efficiency.

In Eq. (3), $t(r)$ is the transmission function of the transparent part of the FZP structure, and it can be specifically expressed as:

$$t(r)=\begin{cases}1, & r_n\le r<r_{n+1}\\ 0, & else\end{cases}, \tag{4}$$

where $r_n=\sqrt{n}\,r_1$ is the radius of zone *n*, $r_{n+1}=\sqrt{n+1}\,r_1$ is the radius of zone *n*+1, and $n=1, 3, 5, \ldots$ is an odd number. By introducing Eq. (3) into Eq. (1), the focusing properties of FZPs with different thicknesses can be obtained by numerical calculations.

According to the classical theory of x-ray FZPs, the highest focusing efficiency that can be reached is approximately 40% when $\frac{2\pi\delta}{\lambda}\tau=\pi$ and $\frac{2\pi\beta}{\lambda}\tau\to 0$ are satisfied. However, in the actual design process, the two conditions are very difficult to satisfy simultaneously. Generally the phase matching of the thickness of an x-ray FZP is the first criterion in the design process.

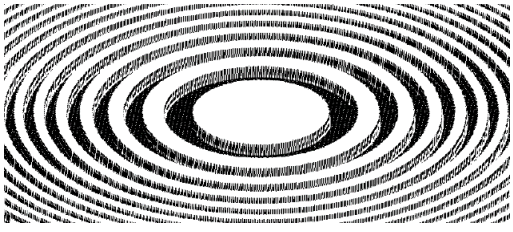

FIG. 2. Image of the structure of an x-ray Fresnel zone plate.

Figure 3 shows the complex refractive index coefficients δ and β as functions of photon energy in the x-ray energy range of 1-10 keV, when the material is Au [16]. When the incident light is 8 keV in energy, it can be found that $\delta=4.77\times10^{-5}$ and $\beta=4.96\times10^{-6}$. Calculations show that the gold film will have a thickness of 0.812, 1.625, and 2.437 μm respectively when the phase shift of the FZP material, given by $\frac{2\pi\delta}{\lambda}\tau$, is equal to π/2, π, and 3π/2. The focusing properties of the focal spot for an FZP film of infinite thickness and with thickness of 0.812, 1.625, and 2.437 μm are given below.

The parameters of the numerical simulations are shown in Table 1. It should be noted that this paper only takes the parameters in Table 1 for example, and FZPs with other parameters can also be calculated by the methods of numerical simulation proposed in this paper, which can be used to guide the design and application of FZPs.

As shown in Fig. 4, the highest focusing efficiency is achieved when the Au FZP's thickness is 1.625 μm. It implies that choosing the appropriate thickness based on the incident wavelength λ is very important to improving the focusing efficiency of the FZP. The full-width-half-maximums of the focal spots are around 100 nm for different film thicknesses, equivalent to the width of the outermost zone Δr. This agrees with the theoretical expectation.

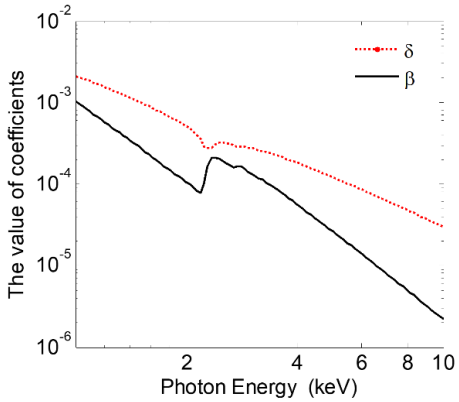

FIG. 3. The relationship between the complex refractive index coefficients and photon energy, for gold.

TABLE 1. The parameters of the FZP for numerical simulations

Incident photon energy	8 keV
The corresponding wavelength	0.155 nm
Selected FZP material	Au
Radius of the first zone	2 μm
Number of half-zone plates	100
Width of the outermost zone	100 nm
Focal length of the FZP	25.8 mm

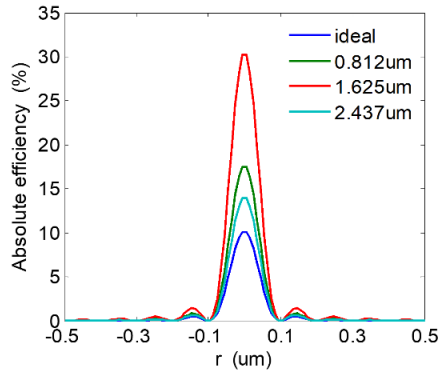

FIG. 4. The focusing efficiency of the FZP for different Au thicknesses.

3.2. The Effects of Incline Angle

Inclination of the sidewall profile is unavoidable in the practice of fabricating FZP samples. The effects of sidewall angle of inclination on the focusing properties are discussed below. For simplicity, here we only consider the case where all sidewalls of the FZP have similar inclinations. The structure of an FZP with sidewall inclination is shown in Fig. 5, where h represents the thickness of the zone plate, θ represents the incline angle of the sidewall, r_1 represents the radius of the first zone, and r_2 represents the radius of the second zone.

Considering the inclination of the sidewall, the transmission function of the transparent parts of the FZP can be expressed as:

$$t(r)=\begin{cases}1, & r_n+h\cdot\tan\theta\le r<r_{n+1}-h\cdot\tan\theta\\ 0, & else,\end{cases} \tag{5}$$

where $r_n=\sqrt{n}r_1$ is the radius of zone n, $r_{n+1}=\sqrt{n+1}r_1$ is the radius of zone n+1, and $n=1, 3, 5, \ldots$ is an odd number. The thickness and radius of the nontransparent parts of the Fresnel zone plate satisfy the following relation:

$$\tau(r)=\begin{cases}h, & r_{n-1}\le r\le r_{n+1}\\ h-\dfrac{(r-r_n)}{\tan\theta}, & r_n\le r\le r_n+h\cdot\tan\theta\\ 0, & r_n+h\cdot\tan\theta\le r\le r_{n-1}-h\cdot\tan\theta\\ h-\dfrac{(r_{n+1}-r)}{\tan\theta}, & r_{n+1}-h\cdot\tan\theta\le r\le r_{n+1},\end{cases} \tag{6}$$

where $r_0=0$ and $n=1, 3, 5, \ldots$ is an odd number. Combining the two expressions above, we can obtain the total transmission function for a Fresnel zone plate with inclined sidewalls:

$$\bar{t}(x,y)=t(x,y)+[1-t(x,y)]\cdot\exp\left[-j\cdot\frac{2\pi\delta}{\lambda}\tau(x,y)\right]\cdot\exp\left[\frac{-2\pi\beta}{\lambda}\tau(x,y)\right]. \tag{7}$$

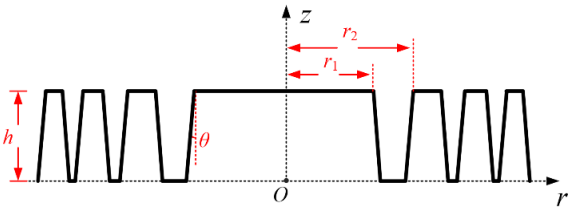

FIG. 5. The structure of an FZP with inclined sidewalls.

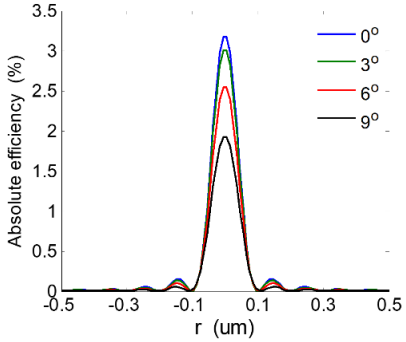

FIG. 6. The focusing efficiency for different inclination angles of the sidewalls.

By introducing Eq. (7) into Eq. (1), the focusing properties of FZPs with different incline angles can be obtained by numerical calculations. Given the thickness of an FZP as 0.3 μm, for example, the influence of the sidewall inclination angle on the focusing properties of the FZP is calculated for similar structural parameters. As shown in Fig. 6, the results of calculation and simulation indicate that the absolute focusing efficiency of the FZP gradually increases with decreasing sidewall inclination angle. This is because the increase of sidewall inclination angle will result in the increase of the opaque part of the zone plate, thus reducing the focusing efficiency of the FZP. To obtain higher absolute focusing efficiency, the inclination of sidewalls should be reduced as far as possible during fabrication. The presence of sidewall inclination has little effect on the size of the focal spot.

3.3. The Effect of Metal Struts

For the FZP to be a self-supporting structure, it is often necessary to add a large number of metal struts in a radial distribution. These intentionally added struts may affect the focusing properties of the FZP, as discussed below.

Figures 7(a) and 7(b) respectively show images of FZPs with regular and random metal struts. In the following numerical simulations, the same calculation parameters as in the first part of this section are selected, and the incline angle of sidewalls is assumed to be zero. Suppose a metal strut is added for every radial angle increment of θ_d, and the angle width of each metal strut is θ_w; then the structure of an FZP with regular metal struts $\tau_2(r,\theta)$ can be expressed as:

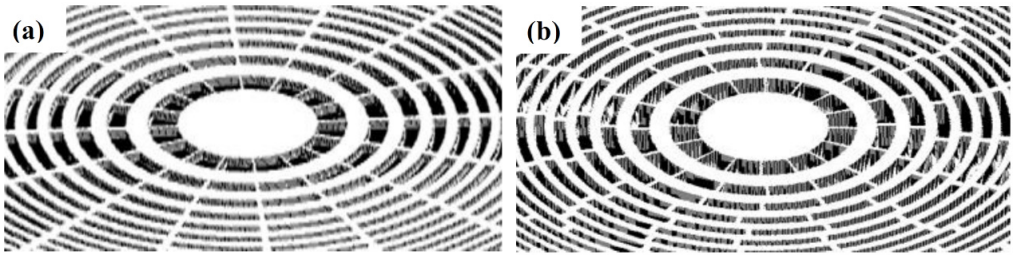

FIG. 7. Fresnel zone plates with (a) regular metal struts and (b) offset metal struts.

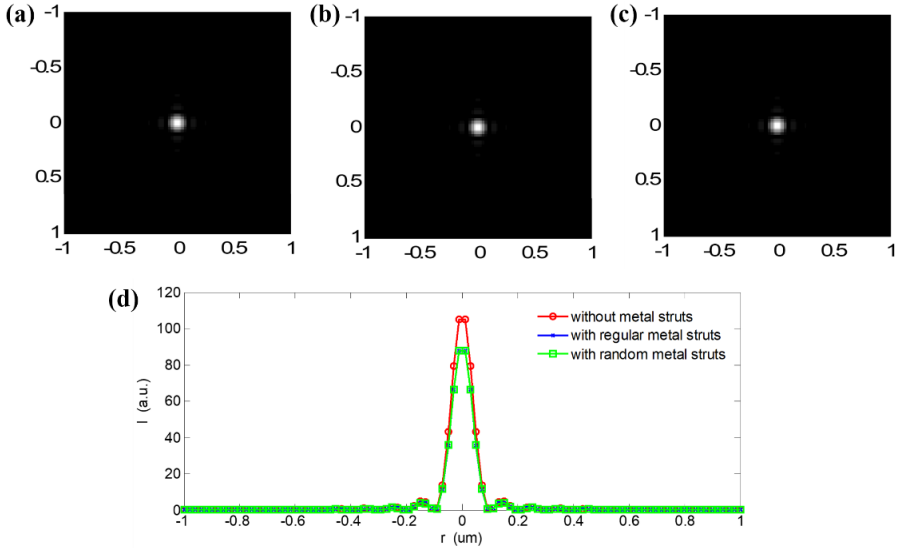

FIG. 8. Focal spots for FZPs (a) without metal struts, (b) with regular metal struts, and (c) with random metal struts, and (d) comparisons of their intensity distributions.

$$\tau_1(r,\theta)=\begin{cases} h, & r_{n-1}\le r<r_n \\ h, & r_n\le r<r_{n+1}, \dfrac{\theta_d-\theta_w}{2}\le \mathrm{mod}(\theta,\theta_d)<\dfrac{\theta_d+\theta_w}{2} \wedge 0, \quad else \end{cases}, \tag{8}$$

where $r_0=0$, $r_n=\sqrt{n}\,r_1$ is the radius of zone n, $r_{n+1}=\sqrt{n+1}\,r_1$ is the radius of zone n+1, $n=1, 3, 5, \ldots$ is an odd number, and $\mathrm{mod}(\theta,\theta_d)$ is the remainder of θ divided by θ_d. In the numerical simulations, we take $\theta_d=22.5°$ and $\theta_w=2°$.

Similarly, the structure of an FZP with random metal struts $\tau_2(r,\theta)$ can be expressed as:

$$\tau_2(r,\theta)=\begin{cases} h, & r_{n-1}\le r<r_n \\ h, & r_n\le r<r_{n+1}, \ p_{(n+1)/2}-\dfrac{\theta_w}{2}\le \mathrm{mod}(\theta,\theta_d)<p_{(n+1)/2}+\dfrac{\theta_w}{2} \wedge 0, \quad else \end{cases}, \tag{9}$$

where $r_0=0$, $r_n=\sqrt{n}\,r_1$ is the radius of zone n, $r_{n+1}=\sqrt{n+1}\,r_1$ is the radius of zone n+1, $n=1, 3, 5, \ldots$ is an odd number, $\mathrm{mod}(\theta,\theta_d)$ is the remainder of θ divided by θ_d, $p_{(n+1)/2}$ is the starting angle of metal struts for the $(n+1)/2^{\text{th}}$ transparent half-wave zone, and is a uniformly distributed random number in the range of $(\frac{\theta_w}{2}, \theta_d-\frac{\theta_w}{2})$.

By introducing Eqs. (8) and (9) into Eq. (7), and then introducing Eq. (7) into Eq. (1), the focusing properties of FZPs with different distributions of metal struts can be obtained by numerical calculations. In numerical simulations, we take $\theta_d=22.5°$ and $\theta_w=2°$.

By numerical simulations, the focusing properties of three kinds of FZP structures (no struts, regular struts, and random struts) are obtained, as shown in Fig. 8. By comparison, it is found that the focal-spot size of an FZP with metal struts is equal to that of the FZP without metal struts, and there is no side-lobe structure in the focal region. Therefore, the presence of metal struts only reduces the light-transmission area of the FZP structure and leads to a decrease of the focusing efficiency, but has little effect on other properties, such as the radius of the focal spot.

3.4. The Effect of Pulse Duration

FZPs can arbitrarily be divided into objective and condenser zone plates. Objective FZPs are applied to form a small focus, generally consist of several hundred zones, and are several hundred nanometers in size. The task of a condenser FZP is to accumulate the maximum possible number of x-ray photons at the focus, and it is characterized

by a large number of zones (N~10^3-10^4). In a theoretical analysis of FZPs, the pulse duration of the incident x-rays is generally not considered. However, in the case of synchrotron radiation or free-electron laser, the pulse width of the x-ray radiation is very short (from femtoseconds to attoseconds). In principle, x-rays are focused with an FZP by a diffraction effect: The incident light passing through different zones (or rings) of an FZP is coherently superimposed at different times. After focusing, the x-ray is concentrated at the focal point. When the incident light is an ultrashort pulse, the focusing properties of an FZP are quite different from those for a long pulse. In the case of a condenser FZP with thousands of zones, to complete time-dependent calculations the complex amplitude superposition of incident x-rays at the same position in the focusing region, but at different times, is considered, and Eq. (1) is appropriately modified as below:

$$U(Q) = \frac{A}{j\lambda}\exp(jkR')\iint_S \sqrt{I(r,t)} \cdot t(S)\left[\frac{\cos(\vec{n},\vec{R}) - \cos(\vec{n},\vec{R'})}{2}\right]\frac{\exp(jkR)}{R}dS, \tag{10}$$

$$I_\tau(r,t) = \exp\left(\frac{-(t-T_\tau)^n}{2\sigma_\tau^n}\right), \tag{11}$$

where $T_\tau = \frac{R'}{c}$ is the time needed to transmit light from a point S to a point Q, t stands for a certain moment in the process of focusing, $t_L = 2\sigma$ is the full-width-half-maximum of the laser pulse, and c is the speed of light. According to the formulas above, the time dependence of the focused light intensity at the focal point (0, 0, f) can be calculated. The pulse durations considered are $t_L = 2$ fs and 10 ps, and the numerical results are shown in Fig. 9. To highlight the effect of pulse duration, the same parameters as in reference [17] are chosen, for the case of a condenser FZP with $N = 41{,}700$ and incident-x-ray wavelength $\lambda = 1$ nm, for numerical calculations.

Figure 9 gives the results for the two cases above. It is found that the FZP elongates the pulse width by $\Delta t = \frac{N\lambda}{(2c)}$. When choosing the related parameters in this paper, $\Delta t = 69.5fs$ can be obtained. As shown in Fig. 9(a), when the incident x-ray pulse width satisfies $t_L \ll \Delta t$, the effect of pulse elongation by the FZP is very obvious and must be considered. As shown in Fig. 9(b), when the pulse satisfies $t_L \gg \Delta t$, the effect can be completely negligible.

IV. CONCLUSION

In this paper, the influences of nonideal factors on the focusing properties of FZPs have been systematically studied by numerical simulations of scalar diffraction theory. In detail, the influence of the thickness on the focusing efficiency was calculated, for a given incident wavelength and material of FZP. It was found that choosing an appropriate thickness based on the incident wavelength λ is very important, and can improve the focusing efficiency of the FZPs.

The diffraction efficiency and size of the focal spot were calculated for different inclination angles of the zone sidewalls. It was found that the absolute focusing efficiency of an FZP increases with decreasing incline angle, but the presence of inclination has little effect on the size of the focal spot. The effect of struts within FZPs (no struts, regularly spaced struts and randomly spaced struts) on the

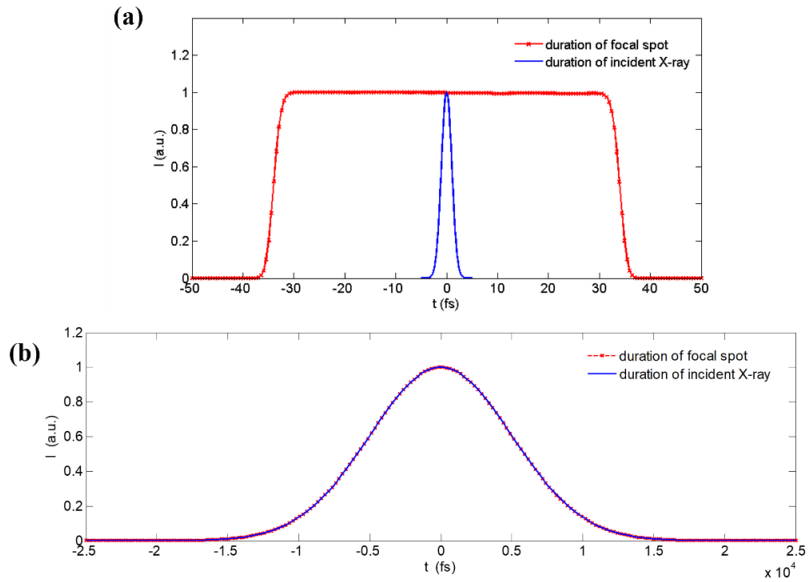

FIG. 9. The pulse duration at the focal spot, produced by incident light with (a) pulse width of 2 fs and (b) pulse width of 10 ps.

focusing properties was discussed, and it was found that the presence of metal struts only reduces the light-transmission area of the FZP structure and leads to decreased focusing efficiency. The struts have little effect on other properties, such as the radius of the focal spot.

The focusing characteristics of an FZP due to incident x-ray pulse duration at the focal spot were studied. It was found that the FZP (especially a condenser FZP) elongates the widths of incident ultrashort x-ray pulses. The work in this paper offers important guidance for design, processing, and application of FZPs.

ACKNOWLEDGMENT

This study was supported by grants from the National Key Research and Development Program of China (Grant No. 2017YFA0206001), the Science Challenging Program (Grant No. JCKY2016212A506-0106), the Science and Technology on Plasma Physics Laboratory at CAEP (Grant No. 6142A0402030317), the Laboratory of Precision Manufacturing Technology at CAEP (Grant No. ZT17003), and the Young Talent Fund of Laser Fusion Research Center (Grant No. LFRC-CZ029).

REFERENCES

1. D. Attwood, *Soft X-ray and Extreme Ultraviolet Radiation: Principles and Applications* (Cambridge University Press, New York, UK, 1999).
2. C. G. Schroer, "Focusing hard x-rays to nanometer dimensions using Fresnel zone plates," Phys. Rev. B **74**, 033405 (2006).
3. J. Reinspach, M. Lindblom, M. Bertilson, O. V. Hofsten, H. M. Hertz, and A. Holmberg, "13 nm high-efficiency nickel-germanium soft x-ray zone plates," J. Vac. Sci. Technol. B **29**, 011012 (2011).
4. K. Jefimovs, O. Bunk, F. Pfeiffer, D. Grolimund, J. F. V. D. Veen, and C. David, "Fabrication of Fresnel zone plates for hard X-rays," Microelectron. Eng. **84**, 1467-1470 (2007).
5. V. V. Lider, "Zone plates for X-ray focusing," J. Surf. Invest.: X-ray, Synchrotron Neutron Tech. **11**, 1113-1127 (2017).
6. J. Vila-Comamala, K. Jefimovs, J. Raabe, T. Pilvi, R. H. Fink, M. Senoner, A. Maasdorf, M. Ritala, and C. David, "Advanced thin film technology for ultrahigh resolution X-ray microscopy," Ultramicroscopy **109**, 1360-1364 (2009).
7. K. Keskinbora, C. Grévent, M. Bechtel, M. Weigand, E. Goering, A. Nadzeyka, L. Peto, S. Rehbein, G. Schneider, R. Follath, J. Vila-Comamala, H. Yan, and G. Schütz, "Ion beam lithography for Fresnel zone plates in X-ray microscopy," Opt. Express **21**, 11747-11756 (2013).
8. I. A. Artyukov, I. N. Bukreeva, V. A. Chernov, R. M. Feshchenko, K. M. Golant, W. Jark, S. V. Lavrishchev, A. N. Mitrofanov, A. V. Popov, and A. V. Vinogradov, "Zone plates for hard X-rays fabricated with the SPCVD technology," Nucl. Instrum. Methods Phys. Res. Sect. A **603**, 66-68 (2009).
9. C. David, B. Nohammer, and E. Ziegler, "Wet etching of linear Fresnel zone plates for hard X-rays," Microelectron. Eng. **61-62**, 987-992 (2002).
10. P. P. Ilinski, B. P. Lai, N. J. Bassom, J. Donald, and G. J. Athas, "X-ray zone plate fabrication using a focused ion beam," Proc. SPIE **4145**, 311-316 (2001).
11. P. Tiwari, P. Mondal, A. K. Srivastava, H. Srivastava, R. Dhawan, and S. Rai, "Fabrication of tungsten Fresnel zone plates for hard x-rays using wet etching," J. Vac. Sci. Technol. B **35**, 051602 (2017).
12. S. Tamura, M. Yasumoto, N. Kamijo, Y. Suzuki, M. Awaji, A. Takeuchi, K. Uesugi, Y. Terada, and H. Takano, "New approaches to fabrication of multilayer Fresnel zone plate for high-energy synchrotron radiation X-rays," Vacuum **80**, 823-827 (2006).
13. Q. Fan, Y. Liu, Z. Yang, L. Wei, Q. Zhang, Y. Chen, F. Hu, C. Wang, Y. Gu, W. Zhou, G. Jiang, and L. Cao, "Focusing single-order diffraction transmission grating with a focusing plane perpendicular to the grating surface," Opt. Express **23**, 16281-16288 (2015).
14. Q. Fan, S. Wang, Z. Yang, L. Wei, F. Hu, H. Zang, Q. Zhang, C. Wang, G. Jiang, and L. Cao, "The realization of long focal depth with a linear varied-area zone plate," J. Mod. Opt. **64**, 244-250 (2016).
15. H. P. Zang, C. K. Wang, Y. L. Gao, W. M. Zhou, L. Y. Kuang, L. Wei, W. Fan, W. H. Zhang, Z. Q. Zhao, L. F. Cao, Y. Q. Gu, B. H. Zhang, G. Jiang, X. L. Zhu, C. Q. Xie, Y. D. Zhao, and M. Q. Cui, "Elimination of higher-order diffraction using zigzag transmission grating in soft x-ray region," Appl. Phys. Lett. **100**, 111904 (2012).
16. Center for X-Ray Optics (CXRO), *Index of Refraction*, (The Center for X-ray Optics, 2010), http://henke.lbl.gov/optical_constants/getdb2.html.
17. W. Chao, E. Anderson, G. P. Denbeaux, B. Harteneck, J. A. Liddle, D. L. Olynick, A. L. Pearson, F. Salmassi, C. Y. Song, and D. T. Attwood, "20-nm-resolution soft x-ray microscopy demonstrated by use of multilayer test structures," Opt. Lett. **28**, 2019-2021 (2003).